2007 IEEE International Conference on
Robotics and Automation
Roma, Italy, 10-14 April 2007

ARMin II – 7 DoF rehabilitation robot: mechanics and kinematics

Matjaž Mihelj
Faculty of Electrical Engineering
University of Ljubljana
Tržaška c. 25, SI-1000 Ljubljana, Slovenia
matjaz.mihelj@robo.fe.uni-lj.si

Tobias Nef and Robert Riener
Sensory-Motor Systems Lab
ETH Zurich and University Zurich
CH-8092 Zurich, Switzerland
[nef, riener]@mavt.ethz.ch

***Abstract*— Task-oriented repetitive movements can improve motor recovery in patients with neurological or orthopaedic lesions. The application of robotics can serve to assist, enhance, evaluate, and document neurological and orthopaedic rehabilitation. ARMin II is the second prototype of a robot for arm therapy applicable to the training of activities of daily living. ARMin II has a semi-exoskeletal structure with seven active degrees of freedom (two of them coupled), five adjustable segments to fit in with different patient sizes, and is equipped with position and force sensors. The mechanical structure, the actuators and the sensors of the robot are optimized for patient-cooperative control strategies based on impedance and admittance architectures. This paper describes the mechanical structure and kinematics of ARMin II.**

***Index Terms*— Rehabilitation robotics, upper extremities, kinematics.**

I. INTRODUCTION

A. Rationale for Movement Therapy

Task-oriented repetitive movements can improve muscular strength and movement coordination in patients with impairments due to neurological or orthopaedic problems. Arm therapy is applied for patients with paretic or paralyzed upper extremities after spinal cord injury or stroke. Several studies prove that arm therapy has positive effects on the rehabilitation progress of stroke patients (see [1], [2], [3], [4] and [5] for review). Such therapy enhances motor function recovery, improves movement coordination as well as generates new motion strategies to cope with activities of daily living (ADLs). Movement therapy serves also to prevent secondary complications such as muscle atrophy, osteoporosis, joint degeneration and spasticity. It was observed that longer training sessions per week and longer total training periods have a positive effect on the motor function. In a meta-analysis comprising nine controlled studies with 1051 stroke patients Kwakkel et al. [6] showed that increased training intensity yields positive effects on neuromuscular function and ADLs. The finding that the rehabilitation progress depends on the training intensity motivates the application of robot-aided arm therapy.

B. Rationale for Robot-Aided Arm Therapy

Manually assisted movement training has several major limitations. The training is labor-intensive, and, therefore, training duration is usually limited by personnel shortage and fatigue of the therapist, not by that of the patient. The disadvantageous consequence is that the training sessions are shorter than required to gain an optimal therapeutic outcome. Finally, manually-assisted movement training lacks repeatability and objective measures of patient performance and progress. In contrast, with automated, i.e. robot-assisted, arm training the duration and number of training sessions can be increased. Long-term automated therapy appears to be the only way to make intensive arm training affordable for clinical use. One therapist may be able to train two or more patients at the same time. Thus, personnel costs can be reduced. Furthermore, the robot provides quantitative measures that enable evaluation of the rehabilitation progress.

Several groups have proposed robots to assist physiotherapy and rehabilitation at both the lower and upper limbs [7], [8], [9], [5], [10]. The devices provide a varying degree of assistance to the patient's movements. On one hand, the robot can passively move a completely paralyzed limb, while on the other hand, it can also provide resistance to the movements of patients in advanced phase of rehabilitation.

C. Requirements for a Rehabilitation Robot

It is important that the robot is adapted to the human limb in terms of segment lengths, range of motion, and the number of degrees of freedom (DoFs). A high number of DoFs allows a broad variety of movements, with many anatomical joint axes involved. To allow the training of ADLs, the robot must be able to position the human hand in any given point in space with an arbitrary orientation. This can be achieved by an end-effector based robot or by an exoskeleton. End-effector based robots are connected with the patient's hand or forearm at one connection point. The kinematics of exoskeleton robots matches that of the human arm. Therefore, the arm can be connected with the exoskeleton at several points. Exoskeleton segments must be of variable length in order to make the robot adaptable to different body sizes. The design of a haptic exoskeleton requires various tradeoffs, which limit the achievable performance of the device. The design choices might limit or affect human motion abilities; selection of sensors and actuators determines the weight of the device, its force/torque output range, stability, and cost. Transmissions used for the actuation change friction and the apparent inertia of the device.

*This work was partially supported by Marie Curie Intra European Fellowship MEIF-CT-2005-010084 to M. Mihelj.

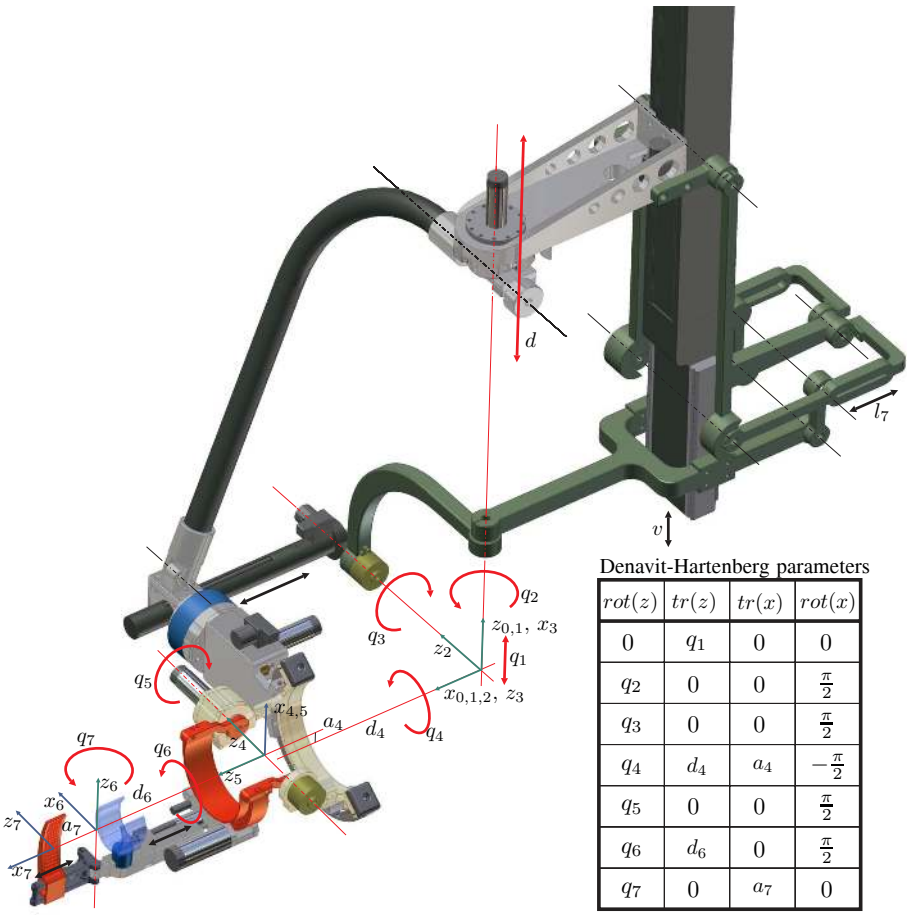

Denavit-Hartenberg parameters

$rot(z)$	$tr(z)$	$tr(x)$	$rot(x)$
0	q_1	0	0
q_2	0	0	$\frac{\pi}{2}$
q_3	0	0	$\frac{\pi}{2}$
q_4	d_4	a_4	$-\frac{\pi}{2}$
q_5	0	0	$\frac{\pi}{2}$
q_6	d_6	0	$\frac{\pi}{2}$
q_7	0	a_7	0

Fig. 1. ARMin II CAD model: red lines indicate axes that correspond to the anatomical axes of the human arm; black lines indicate auxiliary rotation axes of the ARMin robot; blue and green (rotation axes) arrows indicate axes of coordinate frames placed based on the Denavit-Hartenberg notation; black arrows indicate robot size adjustments; lengths d_4, d_6 and a_7 are passively adjustable to accommodate different arm sizes; vertical position of the robot is adjusted by changing v; variable l_7 allows adjustments of the mechanical coupling; with q_i the joint variables are indicated in the table summarizing Denavit-Hartenberg parameters.

II. METHODS

A. Specification of ARMin II

A semi-exoskeleton solution shown in Fig. 1 was selected for the mechanical structure of the robot. It merges advantages of an end-effector and exoskeleton based robots. The patient sits in a wheelchair beneath the robot. His torso is attached to the wheelchair with straps and bands. The end-effector based mechanics enables actuation of two degrees of freedom of the shoulder joint, namely, arm elevation (flexion/extension in the sagittal plane, abduction/adduction in the frontal plane) using a vertically oriented linear drive actuator and arm horizontal flexion/extension using an ordinary rotary actuator. An additional DoF mechanically coupled to the arm elevation actuation enables vertical displacement of the robot arm elevation axis (vertical translation of z_2 along z_0 axis) in order to comply with the natural movement of the patient's upper arm (during the arm elevation the glenohumeral joint is translated forward and upward).

The distal part of the robot is characterized by a four DoFs exoskeletal structure, with the patient's upper and lower arm placed inside orthotic shells. The exoskeletal mechanics actuates upper arm internal/external rotation, elbow flexion/extension, forearm pronation/supination, and wrist flexion/extension. Due to the limited functional importance of the wrist ulnar/radial deviation, this joint is constrained in a neutral position in order to reduce the complexity of the device. Fingers are not obstructed by the mechanics of the forearm exoskeleton, thus, their functionality is fully preserved. As a result either voluntary finger activity or use of functional electrical stimulation for grasping can be considered and additional mechanical extensions are also possible.

The kinematics of the device is shown in Fig 1. The robot coordinate frames were chosen based on the Denavit-Hartenberg (D-H) notation [11]. The table in Fig. 1 summarizes the robot D-H parameters. Joint variables are indicated with q_i. Displacement q_1 and rotation q_3 are coupled through the mechanical linkage. In order to accommodate patients of various sizes, additional four passive DoFs were implemented. Lengths d_4, d_6, and a_7 enable adjustment of the robot to different upper and lower arm segment lengths

as well as hand sizes. Changing v by using an external mechanism sets the vertical position of the robot for different patient heights. The additional variable l_7 enables adjustment of the mechanical coupling transmission ratio and is only meant for experimental purposes in order to find the best relation between joint variables q_1 and q_3.

The mechanism in Fig. 1 is positioned in a configuration where robot links are either parallel or perpendicular. However, it is clear that this can not be achieved for any settings of parameters l_7 and d_4. This configuration was chosen to simplify the analysis of kinematics of mechanical coupling, thus, reducing the complexity of equations in the paper by eliminating the need to include initial joint angles (deviations from 0° or 90°). Therefore, equations in section II-B provide only a particular and not a global solution, but still provide a rather general insight into the end-effector based mechanism kinematics. The calculation approach is the same when searching for a global solution.

B. End-effector Based Mechanics

The first ARMin prototype was built with the shoulder axis of rotation fixed, which resulted in uncomfortable postures for the patient during extensive arm elevations (see [12] and [13] for details). In order to solve this issue several options were considered. One option would be to use a motor in the rotation axis z_2 (see Fig. 1) instead of using the linear drive for arm elevation. A smaller linear drive could then be used for vertical displacement of the arm elevation axis. This solution was not adopted due to the safety considerations – using the linear drive for arm elevation guarantees that the arm does not collapse quickly even in the case of power failure. The second possibility would be to use the linear drive for the arm elevation and a smaller linear drive for the vertical positioning of the arm elevation axis. Again safety issues prevented the implementation of such actuation – in case of a control failure the two drives might act in opposite directions and dislocate the patient's shoulder. Therefore, a mechanical coupling between the shoulder elevation actuation and the shoulder elevation axis was implemented. Such design guarantees safety, because the robot axes always match the human anatomical axes, regardless of the controller malfunction or power failure. The drawback of such coupling is the reduced range of motion of the arm elevation as will be shown later. However, the therapy sessions with ARMin I proved that the resulting reduction of functional movements is not significant for the therapy.

The kinematics of the end-effector based mechanics of the robot is shown in Fig. 2. As already mentioned the initial position of the robot was selected such that all robot links are either parallel or perpendicular (blue sketch). The red sketch indicates the displaced mechanism. The effect of the mechanical coupling on the robot kinematics is analyzed next.

Based on the relations in Fig. 2 the following equations

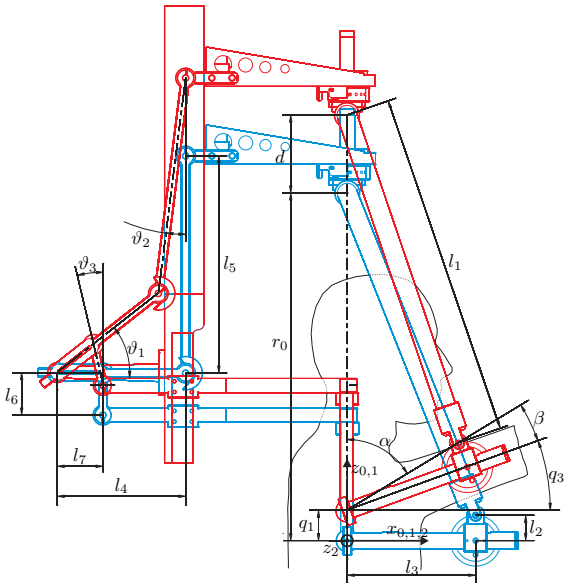

Fig. 2. Kinematic structure of the end-effector based mechanics with the emphasis on passive mechanical coupling between the arm elevation and the vertical position of the center of rotation of the shoulder joint (position of the glenohumeral joint); blue colored sketch indicates the robot in its initial position with all links either parallel or orthogonal; red colored sketch indicates the robot after the displacement from the initial position.

can be written

$$\begin{aligned} l_4 \sin\vartheta_1 &= d + l_5(1-\cos\vartheta_2) \\ l_5 \sin\vartheta_2 &= l_4(1-\cos\vartheta_1). \end{aligned} \tag{1}$$

Solving system (1) for ϑ_1 gives the following result

$$\begin{aligned} \vartheta_1 =& \frac{1}{2l_4\left(l_4^2+(d+l_5)^2\right)} \arccos\Big(l_4\left(2l_4^2+d(d+2l_5)\right) \\ &+ (d+l_5)\sqrt{4l_4^2l_5^2-d^2(d+2l_5)^2}\Big) \quad \Leftarrow \quad d \geq 0 \\ \vartheta_1 =& \frac{-1}{2l_4\left(l_4^2+(d+l_5)^2\right)} \arccos\Big(l_4\left(2l_4^2+d(d+2l_5)\right) \\ &+ (d+l_5)\sqrt{4l_4^2l_5^2-d^2(d+2l_5)^2}\Big) \quad \Leftarrow \quad d < 0. \end{aligned} \tag{2}$$

The vertical displacement of the arm elevation axis is then

$$q_1 = l_6 + l_7\sin\vartheta_1 - \sqrt{l_6^2 - l_7^2(1-\cos\vartheta_1)^2}. \tag{3}$$

Next, arm elevation angle q_3 will be determined. The angle is directly related to the angle α

$$\alpha = \arccos\frac{-l_1^2+l_2^2+l_3^2+(d+r_0-q_1)^2}{2\sqrt{l_2^2+l_3^2}(d+r_0-q_1)}. \tag{4}$$

Since the mechanical coupling is not obligatory from the robot operation point of view, it can also be removed. In this case the arm elevation axis is constrained. Thus, vertical translation q_1 is constant. Setting $q_1 = 0$ simplifies (4) to

$$\alpha = \arccos\frac{-l_1^2+l_2^2+l_3^2+(d+r_0)^2}{2\sqrt{l_2^2+l_3^2}(d+r_0)}. \tag{5}$$

Angle β is constant for each patient. The angle only depends on the constant value l_2 and adjustable length l_3, which

allows adjustment of the robot to different upper arm lengths (variations of D-H parameter $d_4 = l_3 + const.$ in Fig. 1). Thus,

$$\beta = \arctan \frac{l_2}{l_3}. \tag{6}$$

Finally, q_3 can be obtained as

$$q_3 = \frac{\pi}{2} - (\alpha + \beta). \tag{7}$$

Due to the mechanical coupling the range of motion of arm elevation is partially constrained. The mechanical coupling becomes singular in two instances. In the first case links with lengths l_4 and l_5 become collinear. This occurs when the arm is moved upward and the following condition is satisfied

$$l_4^2 + (l_5 + d)^2 = (l_4 + l_5)^2. \tag{8}$$

From here it is possible to calculate the maximal displacement d as

$$d_{max} = -l_5 + \sqrt{l_5(l_5 + 2l_4)} \tag{9}$$

and $q_{1_{max}} = 62$ mm and $q_{3_{max}} = 33°$ from (3) and (7), respectively.

On the other hand, the motion of the arm downward is halted when links with lengths l_6 and l_7 become collinear. This occurs when the following condition is satisfied

$$l_7^2 + (l_6 - q_1)^2 = (l_6 + l_7)^2. \tag{10}$$

The minimal vertical displacement of the elevation axis is then

$$q_{1_{min}} = l_6 - \sqrt{l_6(l_6 + 2l_7)} \tag{11}$$

resulting in $q_{1_{min}} = -33$ mm and $q_{3_{min}} = -47°$. As already noted, these limits are only valid for the configuration of the mechanical coupling as shown in Fig. 3 and need to be recalculated for different values of adjustable lengths l_3 and l_7.

The relations change if the mechanical coupling is removed. The movement of the arm elevation is halted in this case either when $\alpha = 0$, thus,

$$\alpha = 0 \quad \Rightarrow \quad q_{3_{max}} = \frac{\pi}{2} - \beta \tag{12}$$

or when $\alpha = \pi$ resulting in

$$\alpha = \pi \quad \Rightarrow \quad q_{3_{min}} = -\frac{\pi}{2} - \beta. \tag{13}$$

Limits (12) and (13) are only theoretical. The range of motion of arm elevation is more constrained due to the shortness of the linear drive.

The relationship between the arm elevation angle q_3 and the displacements d and q_1 is shown in Fig. 3. The relation is nonlinear. However, such is also the relation between the arm elevation and the vertical movement of the axis of rotation for human arm elevation. Due to the mechanical coupling, the movement of the arm elevation is constrained between $-47° < q_3 < 33°$. This is less than the natural RoM of the human arm. However, the robot workspace is placed in a way to include the most functional part of the workspace of the human upper limb. In order to achieve such arm elevation,

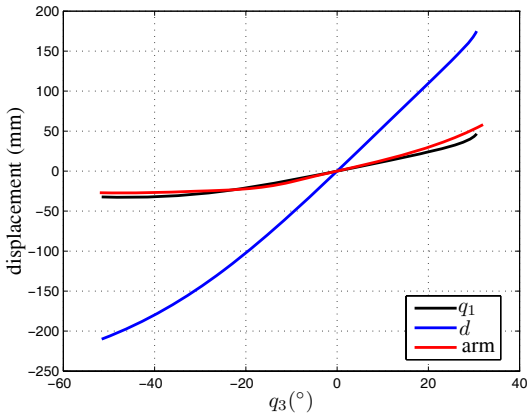

Fig. 3. Displacements d (blue), q_1 (black) and actual vertical displacement of the shoulder axis for the arm elevation (red), depending on the angle of the arm elevation.

the linear drive moves in the 400 mm range. The resulting displacement of the axis of arm elevation is $-33 < q_1 < 62$ mm. This practically corresponds to the measured movement of the human arm elevation axis in the vertical direction (red line). The relation between q_1 and q_3 can be changed by varying distance l_7. Nevertheless, this adjustment is not expected to occur for each patient, but only in the validation phase of the robot.

The actuators of the two DoFs of the end-effector based mechanism need to generate high torques (20 Nm) to support the movement of the human upper limb. The linear drive, which actuates the arm elevation needs to support the weight of the arm against gravity. The linear drive is actuated using a direct current (DC) motor RE 40 (all robot actuators are from Maxon motor ag., Switzerland) coupled directly to the ball spindle axis. The transmission ratio of the ball spindle is high enough (10 mm/revolution), so that no additional gearbox is required. The second axis, the horizontal flexion/extension, is parallel to the gravity vector. Therefore, the actuator does not support the weight of the arm. The actuation is achieved using a DC motor RE 35 and a harmonic drive with a transmission ratio 100:1 (all harmonic drive gearboxes are provided by Harmonic Drive LLC, USA).

C. Exoskeletal Mechanics

The exoskeletal mechanics shown in Fig. 4 comprises 4 active DoFs. The exoskeleton is coupled to the end-effector based mechanism via a force/torque sensor (JR3, Inc., USA). Since all fixations of the human arm to the robot occur in the exoskeleton part, the sensor allows measurement of interaction forces between the upper arm and the robot. An additional force/torque sensor is placed under the forearm cuff to measure interaction forces between the lower arm and the robot. To complete the measurements, the hand cuff will be instrumented with strain-gauges.

The internal/external rotation of the upper arm was build using an of the shelf semi-circular rail and a rail guide (R-Guide, THK co., Ltd., Japan). Four rows of ball circulate

between the rail and the rail guide bearing the load in four directions (radial, reverse-radial and the two lateral directions). A DC motor RE 40 actuates the internal/external rotation via a harmonic drive gearbox (transmission ratio 100:1) and a tooth belt. A cuff made of a soft material is attached to the rail and provides the interface between the robot and the human upper arm. Due to the semi-circular design of the rail, the fixation of the arm to the exoskeleton is quick and easy.

The elbow joint axis is perpendicular to the upper arm internal/external rotation axis. The actuation of the elbow joint is realized using a DC motor RE 35 and a harmonic drive gearbox with a transmission ratio 100:1.

The forearm pronation/supination DoF is custom-designed using a semicircular guide and a cart, which moves along the guide and on which the forearm support structure is attached via a linear guide. The linear guide provides a passive DoF to accommodate the exoskeleton to different forearm lengths. The actuation is achieved using a steel cable wrapped on the outer side of the guide and around the shaft of a motor RE 30 attached to the cart (the steel cable is at the same time wrapped around the shaft of a multi-turn potentiometer). The cart motion is constrained to the semicircular guide by 16 ball bearings as shown on the left side in Fig. 4. The ball bearings are placed such to bear forces in four directions. The only movement allowed is along the semicircular guide. The human forearm is coupled to the exoskeleton through a forearm cuff attached to a force/torque sensor and covered in soft material.

The wrist flexion/extension DoF is implemented using a DC motor RE 25 attached to a high-efficiency ball spindle (Abssac Ltd., UK), which is further connected to a lever system used to transform the linear motion into the rotation around the wrist flexion/extension joint. The hand cuff attaches to the outer side of the hand using a velcro band. Its position is adjustable to accommodate different hand sizes. The movement of the fingers is not obstructed. Therefore, they can be considered for training of ADLs.

All robot axes are backdrivable. However, the friction in most of the joints is considerable due to the use of the harmonic drive gearboxes or ball spindles. The axes are instrumented with high resolution encoders and linear or angular position transducers providing the redundant position information as well as the absolute position reference. The robot bacdrivability in combination with the use of force/torque sensors enables the implementation of impedance or admittance based patient cooperative control strategies.

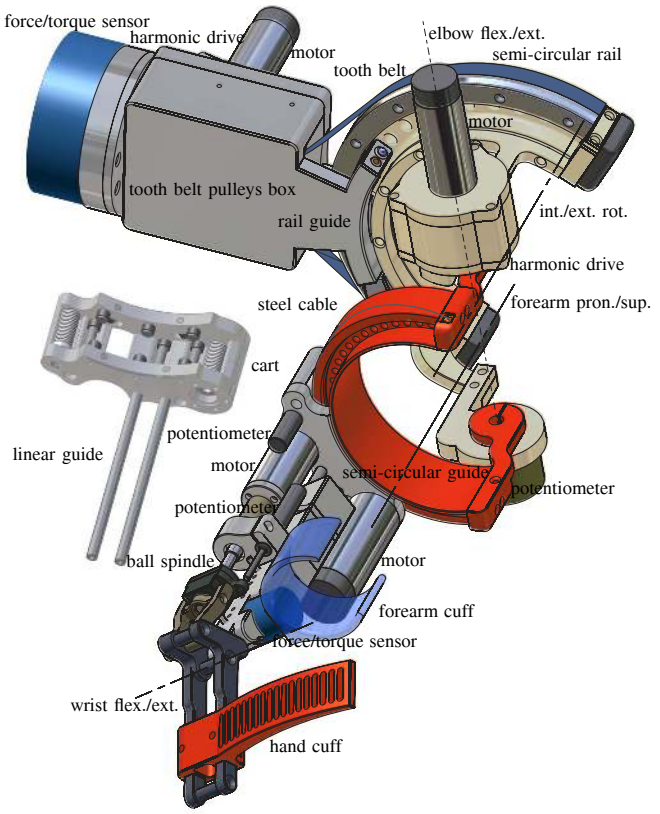

Fig. 4. Exoskeletal mechanics enabling actuation of shoulder internal/external rotation, elbow flexion/extension, forearm pronation/suppination and wrist flexion/extension; the exoskeletal part is coupled to the end-effector based mechanics through a force/torque sensor.

Fig. 5. Subject sitting in a wheelchair is coupled to the ARMin II robot. A physiotherapist sitting near by is selecting the rehabilitation procedure.

III. RESULTS

The ARMin II prototype with a subject being exercised is shown in Fig. 5. A 3D graphical display using a large screen and two overhead projectors as well as a sound system with 6 speakers (not shown in the figure) were added to generate virtual environments for arm rehabilitation. Haptic feedback is provided by the robot. The robot is currently being evaluated with healthy volunteers in order to optimize settings of the mechanical structure and control system. The preliminary results are encouraging. Especially the comfort when using the robot has been significantly increased compared to the first ARMin prototype, due to the vertical movement of the shoulder joint center of rotation. At the same time the robot allows more complex arm movements due to two additional DoFs. Fingers movement is not obstructed by the robot.

Therefore, use of functional electrical stimulation or devices such as Rutgers Master [14] can be considered.

A. Comparison of Human and Robot RoM

The ARMin II robot workspace was chosen such to allow training in the most functional range of human upper limb workspace. Table I summarizes RoM of the human arm and that of the robot. The robot RoM was calculated for the configurations with and without the mechanical coupling between q_1 and q_3. The robot RoM in general matches that of the human arm. A significantly smaller RoM can be observed for the arm elevation, when using ARMin II with the mechanical coupling. However, the RoM was chosen in a way to allow training of majority of ADLs like eating, drinking, combing hair, taking care of personal hygiene, working on a table, etc.

TABLE I

RoM OF THE HUMAN ARM AND ARMIN WITH (ARMIN+MC) AND WITHOUT (ARMIN-MC) THE MECHANICAL COUPLING. VALUES ARE DEFINED BASED ON THE INITIAL ARMIN POSTURE AS SHOWN IN FIG. 1.

Human	Armin+MC	ARMin-MC
$-30 < q_1 < 60\,mm$	$-33 < q_1 < 62\,mm$	$q_1 = 0\,mm$
$-135^\circ < q_2 < 45^\circ$	$-130^\circ < q_2 < 50^\circ$	
$-135^\circ < q_3 < 100^\circ$	$-47^\circ < q_3 < 33^\circ$	$-70^\circ < q_3^* < 45^\circ$
$-140^\circ < q_4 < 5^\circ$	$-120^\circ < q_4 < 5^\circ$	
$0^\circ < q_5 < 135^\circ$	$5^\circ < q_5 < 120^\circ$	
$-90^\circ < q_6 < -90^\circ$	$-70^\circ < q_6 < 70^\circ$	
$-50^\circ < q_7 < 70^\circ$	$-35^\circ < q_7 < 50^\circ$	

* limited by the length of the linear drive

B. Passive and Active Safety

Passive safety features, for example no sharp edges in mechanical construction and mechanical end-stops to guarantee that no joint can exceed the anatomical range of motion of the human limb, are combined with active safety features. Redundant absolute position sensing potentiometers allow detection of malfunction of a position sensor or a controller. Surveillance routines implemented in the software include current and speed monitoring, a collision detection algorithm and several watchdog systems. A dead-man button must always be enabled by the physiotherapist.

Whenever an abnormal event is detected, the safety circuit immediately cuts the power of the motor drives. As the robot is designed with a passive weight compensation system (pulley, rope, and counterweight) it does not collapse after power loss. Since all drives are backdrivable, the robot can be moved manually by a therapist in order to release the patient from a potentially uncomfortable or dangerous position.

IV. SUMMARY AND CONCLUSIONS

The rehabilitation system was designed to positively influence the outcome of the rehabilitation period through more effective therapy especially by motivating the patient with a multimodal display and his active involvement in the therapy.

In order to assess the quality of the recovery, objective measures are required. Like many other clinical measures, functional recovery is presently measured using subjective scales. The proposed automated rehabilitation system not only enables enhanced rehabilitation but also provides assessment of the progress of rehabilitation in terms of specific and objective performance indices expressed as numeric values easy to understand to clinicians. Force/torque as well as position/velocity data are available for the analysis.

The ARMin robot that was built with four active DoFs in the first prototype has now been extended with two additional DoFs for the forearm in order to allow training of ADLs and an additional DoF to accommodate the vertical movement of the center of rotation of the shoulder joint. The modular design of the ARMin robot that allows various combinations of proximal and distal arm training modes will also provide the platform for the search of the best rehabilitation practice.

REFERENCES

[1] T. Platz, "Evidenzbasierte Armrehabilitation: Eine systematische Literaturübersicht," *Nervenarzt*, vol. 74, pp. 841–849, 2003.

[2] P. S. Lum, C. G. Burgar, P. C. Shor, M. Majmundar, and M. van der Loos, "Robot-assisted movement training compared with conventional therapy techniques for the rehabilitation of upper limb motor function after stroke," *Arch. Phys. Med. Rehabil.*, vol. 83, pp. 952–959, 2002.

[3] E. M. Frick and J. L. Alberts, "Combined use of repetitive task practice and an assistive robotic device in a patient with subacute stroke," *Physical Therapy*, vol. 86, pp. 1378–1386, 2006.

[4] D. Reinkensmayer, J. L. Emken, and S. C. Cramer, "Robotics, motor learning, and neurological recovery," *Annu. Rev. Biomedical. Eng.*, vol. 6, pp. 497–525, 2004.

[5] R. Riener, T. Nef, and G. Colombo, "Robot-aided neurorehabilitation for the upper extremities," *Medical & Biological Engineering & Computing*, vol. 43, pp. 2–10, 2005.

[6] G. Kwakkel, R. Wagenaar, T. Koelman, G. Lankhorst, and J. Koetsier, "Effects of intensity of rehabilitation after stroke. a research synthesis," *Stroke*, vol. 28, pp. 1550–1556, 1997.

[7] M. Bergamasco, B. Allotta, L. Bosio, L. Ferretti, G. Parrini, G. M. Prisco, F. Salsedo, and G. Sartini, "An arm exoskeleton system for teleoperation and virtual environments applications," *Proceedings of the 1994 IEEE International Conference on Robotics & Automation, San Diego, California, USA*, pp. 1449–1454, 1994.

[8] W. S. Harwin and T. Rahman, "Analysis of force-reflecting telerobotic system for rehabilitation applications," in *Proceedings of the 1st European Conference on Disability, Virtual Reality and Associated Technologies*, Maidenhead, UK, 1996, pp. 171–178.

[9] H. I. Krebs, N. Hogan, M. L. Alisen, and B. T. Volpe, "Robot-aided neurorehabilitation," *IEEE Transactions Rehabilitation Engineering*, vol. 6, pp. 75–87, 1998.

[10] A. Gupta and M. K. O'Malley, "Design of a haptic arm exoskeleton for training and rehabilitation," *IEEE/ASME Trans. Mechatron.*, vol. 11, pp. 280–289, 2006.

[11] J. Denavit and R. S. Hartenberg, "A kinematic notation for lower-pair mechanisms based on matrices," *ASME Journal of Applied Mechanics*, vol. 23, pp. 215–221, 1955.

[12] T. Nef, M. Mihelj, G. Colombo, and R. Riener, "Armin - robot for rehabilitation of the upper extremities," *Proceedings of the 2006 IEEE International Conference on Robotics & Automation, Orlando, Florida, USA.*, pp. 3152–3157, 2006.

[13] M. Mihelj, T. Nef, and R. Riener, "Armin - toward a six dof upper limb rehabilitation robot," in *IEEE / RAS-EMBS International Conference on Biomedical Robotics and Biomechatronics*, Pisa, Italy, 2006.

[14] M. Bouzit, G. Burdea, G. Popescu, and R. Boian, "The Rutgers Master II-new design force-feedback glove," *IEEE/ASME Transactions on Mechatronics*, vol. 7, pp. 256–263, 2002.